

See discussions, stats, and author profiles for this publication at: <https://www.researchgate.net/publication/239590484>

# Advanced Space Propulsion Based on the Flow-Stabilized Z-Pinch Fusion Concept

Article · July 2006

DOI: 10.2514/6.2006-4805

CITATIONS

7

READS

2,406

7 authors, including:



[Uri Shumlak](#)

University of Washington Seattle

236 PUBLICATIONS 1,718 CITATIONS

[SEE PROFILE](#)



[Robert Lilly](#)

Air Force Research Laboratory

16 PUBLICATIONS 57 CITATIONS

[SEE PROFILE](#)



[Colin Stuart Adams](#)

Virginia Polytechnic Institute and State University

29 PUBLICATIONS 192 CITATIONS

[SEE PROFILE](#)



[Raymond P. Golingo](#)

Fuse Energy

81 PUBLICATIONS 403 CITATIONS

[SEE PROFILE](#)

Some of the authors of this publication are also working on these related projects:



Fuse diagnostics [View project](#)



Plasma Catalysis [View project](#)

# Advanced Space Propulsion Based on the Flow-Stabilized Z-Pinch Fusion Concept

U. Shumlak\*, R. C. Lilly,<sup>†</sup> C. S. Adams,<sup>‡</sup> R. P. Golingo,<sup>§</sup> S. L. Jackson,<sup>¶</sup>  
S. D. Knecht,<sup>||</sup> and B. A. Nelson\*\*

*Aerospace & Energetics Research Program, University of Washington, Seattle, Washington 98195-2250*

A fusion space thruster based on the flow-stabilized Z-pinch may be possible in the near-term and provide many advantages over other fusion-based thruster concepts. The Z-pinch equilibrium is classically unstable to gross disruption modes according to theoretical, numerical, and experimental evidence. However, a new stabilization mechanism has been discovered that can stabilize these modes with plasma flow. The stabilizing mechanism was developed for a Z-pinch plasma equilibrium which has an axial velocity profile that is linear in radius. When the velocity shear exceeds a threshold, the plasma modes are stabilized. The magnitude of the peak velocity is dependent on the mode wavelength but is sub-Alfvénic for the wavelengths of experimental interest,  $v_{max} > 0.1V_Aka$  where  $V_A$  is the Alfvén speed,  $k$  is the axial wave vector, and  $a$  is the characteristic pinch radius. The flow Z-pinch experiment ZaP has been built at the University of Washington to experimentally verify the sheared flow stabilizing mechanism. The experiment has achieved plasma flow velocities of  $10^5 m/s$  and stability for almost 2000 growth times. For more information the reader is encouraged to visit <http://www.aa.washington.edu/AERP/ZaP>. The extension of the flow Z-pinch to a space thruster is straight forward. The plasma in a flow Z-pinch would already be moving axially, fusing, and releasing a tremendous amount of nuclear energy. The end of the Z-pinch can be left open to allow the escape of the energetic plasma. Specific impulses in the range of  $10^6 s$  and thrust levels of  $10^5 N$  are possible.

## Nomenclature

$r$	Radial coordinate, m
$a$	Characteristic pinch radius, mm
$L$	Pinch length, m
$\mathbf{j}$	Current density, A/m <sup>2</sup>
$I$	Current, MA
$\mathbf{B}$	Magnetic flux density, T
$p$	Pressure, Pa

\*Associate Professor, Aeronautics & Astronautics, AIAA Senior Member.

<sup>†</sup>Graduate Student, Aeronautics & Astronautics, AIAA Student Member.

<sup>‡</sup>Graduate Student, Aeronautics & Astronautics, AIAA Student Member.

<sup>§</sup>Research Associate, Aeronautics & Astronautics.

<sup>¶</sup>National Research Council Associate, Naval Research Laboratory, AIAA Member.

<sup>||</sup>Graduate Student, Aeronautics & Astronautics, AIAA Student Member.

\*\*Research Associate Professor, Electrical Engineering.

Copyright © 2006 by the American Institute of Aeronautics and Astronautics, Inc. The U.S. Government has a royalty-free license to exercise all rights under the copyright claimed herein for Governmental purposes. All other rights are reserved by the copyright owner.

$n$	Number density, $\text{m}^{-3}$
$T, T_e, T_i$	Total, electron, ion temperatures, keV
$k$	Axial wave vector, $\text{m}^{-1}$
$m$	Azimuthal mode number
$\Gamma$	Ratio of specific heats
$\beta$	Ratio of plasma to magnetic pressures
$v$	Plasma flow velocity, m/s
$V_A$	Alfvén speed, m/s, $(=B/\sqrt{\mu_o\rho})$
$v_e$	Jet exhaust velocity, m/s
$\eta$	Resistivity, $\Omega\text{-m}$
$\dot{m}$	Mass flow rate, kg/s
$P_{in}$	Input power, W
$P_f$	Fusion power, W
$Q$	Fusion power gain ratio $(=P_f/P_{in})$
$\tau$	Plasma confinement time, s
$\mu_o$	Permeability of free space, $(=4\pi \times 10^{-7})$

## I. Introduction

Nuclear fusion energy holds the promise of enabling human exploration of the outer solar system, and perhaps beyond. However, scientific and technical challenges must be surmounted before a fusion-based space thruster will become reality. These challenges center on stable plasma configurations, and primarily plasma configurations that have a sufficiently low mass for space applications.

This paper presents recent plasma research that shows a pure Z-pinch can be stabilized. The Z-pinch discussed in this paper is a pure Z-pinch and not a screw pinch. No external magnetic fields are applied. A stable Z-pinch has many advantages over other magnetic confinement configurations. External magnetic field coils are not needed to provide plasma stability, and the compressing magnetic field only needs to compress the plasma and not the stabilizing magnetic field. For space applications this represents a tremendous weight and recirculating power savings.

## II. Z-Pinch Equilibrium and Instabilities

The Z-pinch equilibrium is the simplest magnetic confinement configuration possible. It consists of a plasma column with an axial electrical current which produces an azimuthal magnetic field. The Lorentz force ( $\mathbf{j} \times \mathbf{B}$ ) confines and compresses the plasma. The equilibrium is described by the radial force balance,

$$(\mathbf{j} \times \mathbf{B})_r = (\nabla p)_r, \quad (1)$$

or substituting Ampere's law for the current gives

$$\frac{B_\theta}{\mu_o r} \frac{d(rB_\theta)}{dr} + \frac{dp}{dr} = 0. \quad (2)$$

The magnetic pressure balances the plasma pressure.

Z-pinch plasmas have been investigated since the beginning of magnetic confinement fusion research. The Z-pinch magnetic confinement configuration has many overlapping research issues with the arcjet thruster. They both use the same simple equilibrium and have the same stability issues. Unfortunately, the simple equilibrium given by Eq.(2) is unstable to gross disruption modes which have been seen theoretically and experimentally.<sup>1</sup>

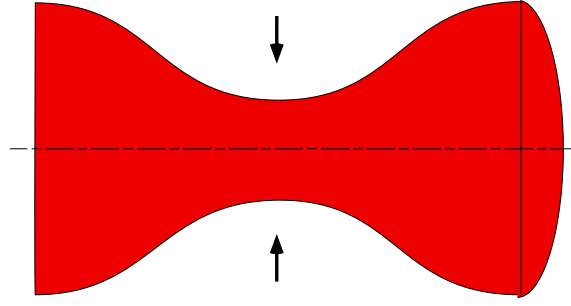


**Figure 1.** Schematic representation of the sausage ( $m=0$ ) mode in a Z-pinch showing the axisymmetric perturbation which grows exponentially.

### A. Sausage Instability

The plasma column can undergo a sausage ( $m=0$ ) instability. The sausage instability is an axisymmetric displacement of the plasma radius. See Fig. 1. Since the magnetic field varies like  $1/r$  at the plasma/vacuum interface, the magnetic force varies like  $1/r^2$ . The magnetic force is larger where the plasma radius has decreased and smaller where the plasma radius has increased. The instability grows exponentially until the axial plasma current is disrupted which quenches the plasma.

The sausage mode can be stabilized by placing a close-fitting conducting wall close to the pinch plasma. When the instability tries to grow, the wall produces image currents which stabilize the mode. (The constrictor serves this role in arcjet thrusters.) A close-fitting wall is incompatible with fusion plasmas because it precludes the high plasma temperatures required for fusion.

A stability condition against the sausage mode can be found by applying a functional minimization method (or energy principle) to the linear MHD equations.<sup>2</sup> For the sausage mode the linear analysis gives the stability condition

$$-\frac{d \ln p}{d \ln r} \leq \frac{4\Gamma}{2 + \Gamma\beta} \quad (3)$$

where  $\beta = 2\mu_0 p/B^2$  is a local measure of the ratio of plasma pressure to magnetic pressure. This condition must be satisfied everywhere in the plasma for stability against the  $m = 0$  mode. The sausage mode can be stabilized if the pressure does not fall off too rapidly. However, tailoring the pressure profile cannot stabilize the kink instability.

### B. Kink Instability

The plasma column can undergo a kink ( $m=1$ ) instability. The kink instability is an asymmetric displacement of the plasma column. See Fig. 2. When the plasma kinks the magnetic field intensity increases on the inner portion of the bend and decreases on the outer portion of the bend. The corresponding magnetic force causes the instability to continue and grow exponentially.

The kink instability can also be stabilized by placing a conducting wall (constrictor) in close proximity to the plasma column, but as stated, this method is unacceptable for fusion plasmas.

The kink instability can also be stabilized by embedding an axial magnetic field into the plasma. As the plasma kinks, the axial field stretches and resists further kinking. The condition for stability against the kink mode is found by applying an energy principle and is called the Kruskal-Shafranov limit.<sup>3,4</sup>

$$\frac{B_\theta}{B_z} < \frac{2\pi a}{L}. \quad (4)$$

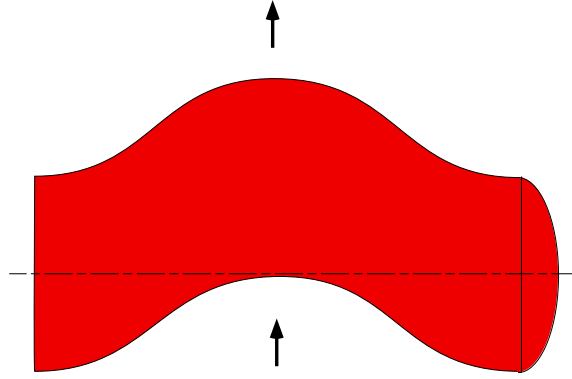


**Figure 2. Schematic representation of the kink ( $m=1$ ) mode in a Z-pinch showing the asymmetric perturbation which grows exponentially.**

This condition limits the plasma current and the plasma pressure that can be stably achieved in a Z-pinch. The equilibrium is now modified so that the radial force of the azimuthal magnetic field balances the plasma pressure and the magnetic pressure of the axial field. A preferred approach would be to stabilize the z-pinch without limiting the plasma current, thereby, allowing high plasma pressure. Additionally, the axial magnetic field transforms the circular azimuthal field lines into helical field lines that thread the plasma and the electrodes. The plasma can then lose heat by thermal conduction parallel to the magnetic field lines. Parallel heat conduction is much larger than perpendicular heat conduction.

### C. Flow Stabilization

A stabilization mechanism has been discovered that can stabilize the unstable modes of a Z-pinch by using plasma flow.<sup>5-8</sup>

The stabilizing mechanism was developed for a Z-pinch plasma equilibrium which has an axial velocity profile that is linear in radius. Magnetohydrodynamics (MHD) theory is applied and a linear stability analysis is performed. The stability analysis confirms the known stabilizing effect of a conducting wall. However, an additional result shows that a velocity shear threshold exists. When the velocity shear exceeds the threshold, the plasma modes are stabilized. The magnitude of the peak velocity is dependent on the mode wavelength but is sub-Alfvénic for the wavelengths of experimental interest even in the no-wall limit.

$$v_{max} > 0.1V_Aka \quad (5)$$

where  $V_A$  is the Alfvén speed,  $k$  is the axial wave vector, and  $a$  is the characteristic pinch radius.<sup>5</sup> The stability results are shown in Fig. 3.

The stabilizing mechanism can perhaps be best understood as an effective mode mixing that occurs when the plasma flow is sheared. As either the sausage or kink instability begins to grow, the shear in the flow mixes the axial locations of the mode. The mixing destructively interferes with the growth of the mode, and the mode is stabilized. A similar stabilizing mechanism has been found when theoretically investigating the classical Rayleigh-Taylor/Kelvin-Helmholtz instabilities.<sup>9</sup>

Nonlinear simulations have been performed and support the sheared flow stabilizing effect in Z-pinch plasma equilibria. The simulations are performed with the Mach2 code<sup>10</sup> which uses the time-dependent, resistive, 2D MHD model. An equilibrium is initialized which has a sheared axial plasma flow and an axially periodic density perturbation. The figure shows the pressure contours for the cases of no flow and  $v_z/a = 0.2kV_A$  at the same times in the simulation. Fig. 4 shows a well developed  $m=0$  instability in a static

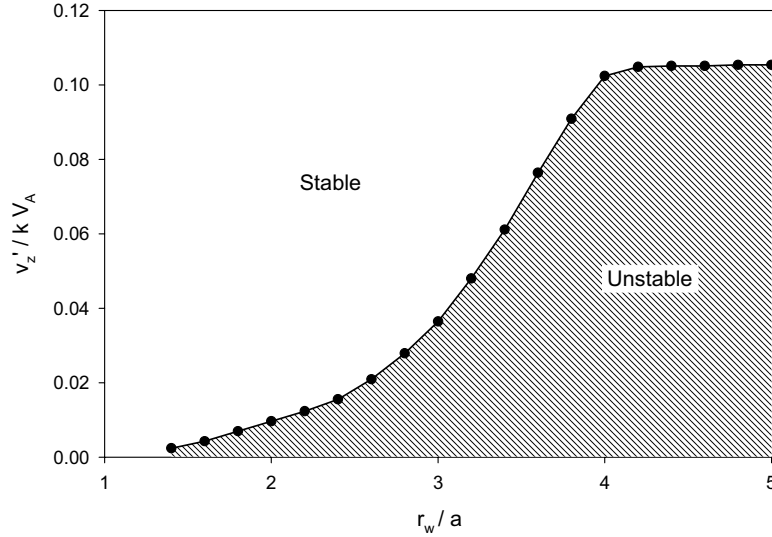


**Figure 3. Linear stability results for a Z-pinch with a sheared axial flow. The stabilizing effect of a conducting wall is evident when the wall is close to the pinch radius. A stability threshold is seen at a normalized velocity shear of approximately 0.1 in the no-wall limit.**

Z pinch plasma and a substantially less developed  $m=0$  instability in a Z pinch plasma with a sheared axial flow.

### III. The Flow Z-Pinch Experiment, ZaP

A flow Z-pinch experiment ZaP has been built at the University of Washington to experimentally verify the sheared flow stabilizing mechanism.<sup>11</sup> The experiment is designed to generate a Z-pinch plasma with a large axial flow by coupling a coaxial acceleration region to an assembly region. A machine drawing of the ZaP experiment is shown in Fig. 5 identifying the relevant features. The experiment is initiated by the injection of neutral gas, usually hydrogen, with fast puff valves into the annular region between the coaxial electrodes located in the middle of the 1 m coaxial acceleration region. An electrical potential is applied across the coaxial electrodes, ionizing the neutral gas, and accelerating the plasma. When current flows through the plasma, the Lorentz force ( $\mathbf{j} \times \mathbf{B}$ ) from the current and the self-field accelerates the plasma axially. When the plasma reaches the end of the coaxial acceleration region, the plasma along the inner electrode moves radially inward and assembles along the axis in the 1 m long assembly region. The plasma along the outer electrode continues to move axially and radially inward during the assembly of the Z-pinch. The plasma finally connects between the end of the inner electrode and the outer electrode end wall forming a complete Z-pinch. Inertia maintains the plasma flow state, and plasma is continually exiting from the coaxial accelerator and assembles into the pinch. The plasma parameters are shown in Table 1.

An azimuthal array of eight equally-spaced, surface-mounted magnetic probes are installed in the outer electrode at the pinch midplane. The probes measure the azimuthal magnetic field at the surface of the outer electrode. The magnetic field values from the probe array are Fourier analyzed to determine the evolution of the low order azimuthal modes ( $m=1,2,3$ ) of the Z-pinch plasma. Data are plotted in Fig. 6 showing the time evolution of the normalized  $m=1,2,3$  Fourier modes of the magnetic field. The figure also shows the evolution of the plasma current for reference.

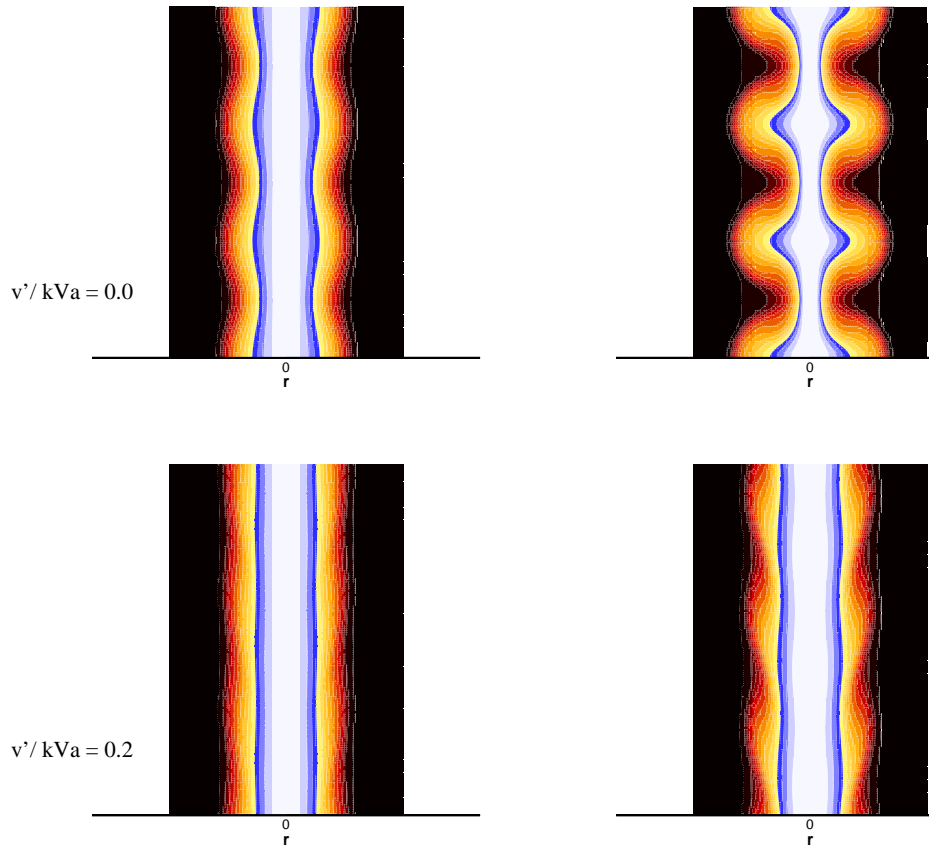


Figure 4. Nonlinear evolution of the sausage mode for a static Z-pinch equilibrium (top images) and one with a sheared axial flow (lower images). Shown are pressure contours.

Table 1. Experimental Parameters of the ZaP Experiment

Entity	Value
Accelerator Length	1 m
Inner Electrode O.D.	0.1 m
Outer Electrode I.D.	0.2 m
Peak Current	0.3 MA
$n$	$10^{22}$ – $10^{23} \text{ m}^{-3}$
$a$	10 mm
$L$	1 m
$T_e + T_i$	0.15–0.25 keV

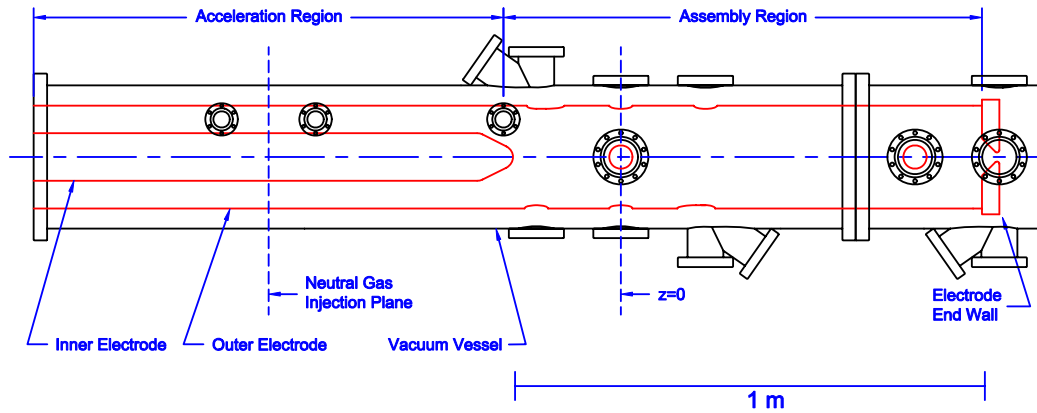


Figure 5. Side view machine drawing of the ZaP experiment showing the relevant features. The vertical ports in the assembly region are used for spectroscopy. The horizontal ports are used for interferometry and visible imaging with a fast framing camera. A “1 m” scale is included for reference.

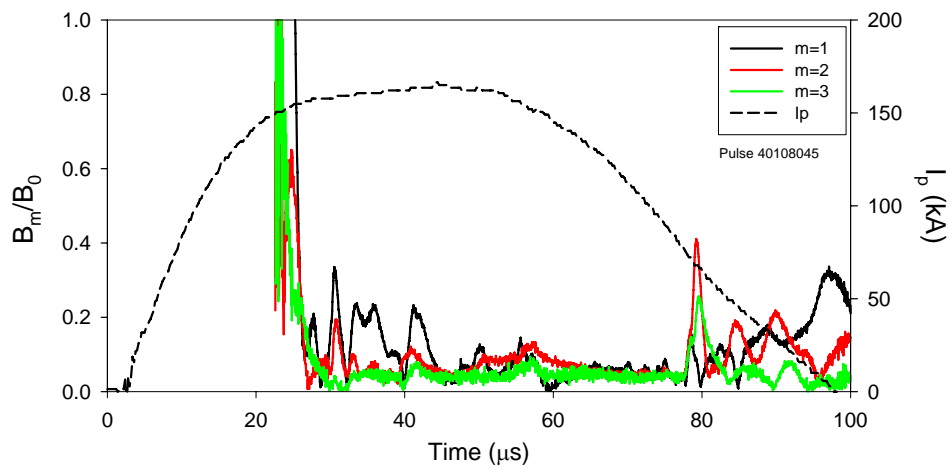


Figure 6. Time evolution of  $m=1,2,3$  Fourier components of the magnetic field fluctuation at  $z=0$  showing the quiescent period from 42  $\mu\text{sec}$  to 79  $\mu\text{sec}$ . The values are normalized to the average magnetic field value at the pinch midplane. The evolution of the plasma current (dashed curve) is included for reference.



The magnetic fluctuation levels of the asymmetric modes are high when the Z-pinch plasma is assembling. After the pinch has formed the fluctuation levels change character for approximately 37  $\mu$ s, from 42 to 79  $\mu$ s. The change in character is identified by lower levels and decreased frequency for the fluctuations. After this quiescent period the fluctuation levels then again change character, increase in magnitude and frequency, and stay high until the end of the plasma pulse. Fluctuations of the normalized  $m=1$  component as presented correspond to a current displacement of  $2\xi/r_w$ . Therefore, a value of  $B_1/B_0 = 0.2$  represents a radial displacement of the current of 10 mm. The 0.2 value defines the quiescent period. These results are consistent with other diagnostic measurements.

The axial velocity profiles are determined during the plasma pulse by measuring the Doppler shift of impurity line radiation with an intensified CCD detector and an imaging spectrometer viewing the plasma through the oblique view port.<sup>6</sup> The exposure times are typically 0.1 - 0.5  $\mu$ s. The chord-integrated data are then deconvolved to determine axial velocity profiles.<sup>12</sup> By varying the recording time between pulses, an evolution of the velocity profile can determine. These data are shown in Fig. 7 as a function of normalized time,  $\tau$ . Time is normalized to the quiescent period (defined as  $\tau = [0,1]$ ) to allow accurate comparison. The magnetic field fluctuations from Fig. 6 are shown in the lower plot of Fig. 7 to provide comparison between fluctuation levels and flow shear.

During the pinch assembly the magnetic fluctuation levels are high and the plasma axial velocity profile is uniform with a value of approximately  $10^5$  m/s. During the quiescent period the magnetic fluctuation level is low and the plasma axial velocity is sheared with either a large velocity at the edge and a low velocity in the plasma core or a low velocity at the edge and a large velocity in the plasma core. After the quiescent period the magnetic fluctuation levels are high and the plasma axial velocity profile is uniform and low.

For the experimental plasma parameters the growth rate of the kink mode in a static plasma is 21 ns. The experimental results show a stable period which is almost 2000 exponential growth times. Experimental evidence suggests there may be an operational mode where the flow Z-pinch reaches a quasi steady-state. For more information on the ZaP experiment the reader is encouraged to read the referenced articles and to visit <http://www.aa.washington.edu/AERP/ZaP>.

## IV. Flow-Stabilized Z-Pinch Fusion Space Thruster

The extension of the flow-stabilized Z-pinch to a space thruster is straight forward. See Fig. 8 for a schematic. The plasma in a flow-stabilized Z-pinch is already moving axially, fusing, and releasing a tremendous amount of nuclear energy. The end of the Z-pinch can be left open to allow the escape of the energetic plasma composed of the fusion products.

The core of the plasma would be at fusion temperatures and should not contact any solid material. The electrodes would flair at the ends to allow the plasma to cool before contact as shown in Fig. 8. The plasma would expand from the fusion heat and propagate into the electrode. This component of the plasma would be sent to a direct energy converter to capture the plasma velocity directly as electrical current. The converted current could also supply power for a magnetic nozzle to improve the conversion of thermal to directed kinetic energy of the fusion products. The power from the direct energy converter could also be used to maintain the circulating plasma current and supply spacecraft power.

Since no external magnetic fields are required to provide plasma stability, the required mass is dramatically reduced compared to other magnetic confinement fusion concepts.

### A. Scaling Relations for the Flow-Stabilized Z-Pinch

Scaling relations are useful to determine the size of thruster required to match the requirements for any mission. The total fusion power scales as

$$P_f \propto \frac{I^4 L}{a^2 T^2} \quad (6)$$

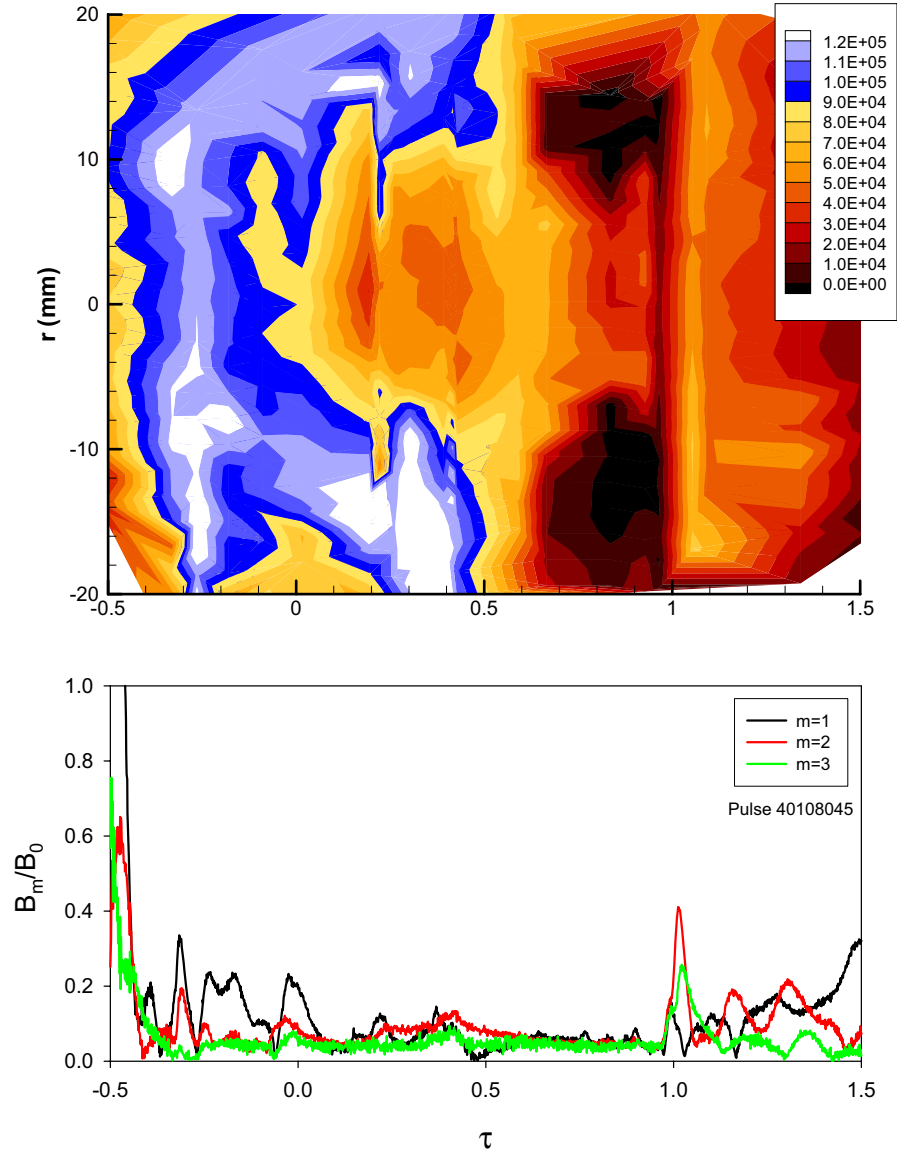


Figure 7. The upper plot shows the plasma axial velocity contours based on the C-III line at 229.7 nm as a function of plasma radius and time. Velocity profiles are recorded once during each pulse. By varying the recording time between pulses, an evolution of the velocity profile can determine. The times are normalized to the quiescent period (defined as [0,1]) to allow accurate comparison. The magnetic field fluctuations from Fig. 6 are shown in the lower plot to provide comparison between fluctuation levels and flow shear.

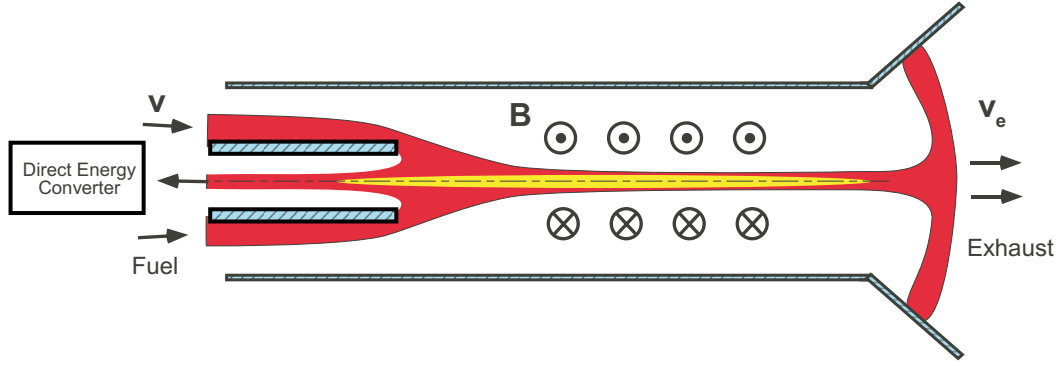


Figure 8. Schematic representation of a flow-stabilized Z-pinch fusion space thruster.

for plasma temperatures high enough that the fusion cross-section is approximately constant.<sup>13,14</sup> Energy must be provided to generate the stabilizing shear flow and the resistive dissipation within the plasma.

$$P_{in} = 1/2 \dot{m}_{fuel} v_{in}^2 + I^2 \eta L / \pi a^2 \quad (7)$$

A significant advantage of the Z-pinch is the high plasma density that is obtained. (In the ZaP experiment peak densities of  $10^{23} \text{ m}^{-3}$  and higher are measured.) The plasma density varies as

$$n \propto \frac{I^2}{a^2 T}. \quad (8)$$

The high density avails the more attractive fusion reactions that generate fewer neutrons, like  $D - He^3$ , or are completely aneutronic, such as  $p - B^{11}$ . The reaction with the highest cross-section is  $D - T$ , but it produces one neutron per reaction that must be shielded. The  $D - He^3$  reaction does not produce any neutrons, but two  $D$  ions can react and produce a neutron. Shielding against neutrons significantly increases the required mass of the spacecraft.

## B. Sample Thruster Parameters

Table 2 lists thruster parameters for a Z-pinch fusion space thruster that could use  $D - He^3$  or  $p - B^{11}$  for fuels. Any temperature below approximately 50 keV effectively precludes the use of  $p - B^{11}$  because the reaction cross-section decreases rapidly, though a lower temperature for  $D - He^3$  will produce a more optimized design because of the resulting higher density. Additional propellant mass may be added to the exhaust plume to generate a higher thrust and lower specific impulse. The thruster parameters are more restrictive for the  $p - B^{11}$  reaction because of the lower reaction cross-section.

The length of the pinch is set by satisfying a complete burn criteria.

$$L \geq v_{in} \tau \quad (9)$$

and  $n\tau > 3 \times 10^{20} \text{ s/m}^3$  for  $D - He^3$  and  $n\tau > 6 \times 10^{21} \text{ s/m}^3$  for  $p - B^{11}$ . The volumetric power is much lower for  $p - B^{11}$  than for  $D - He^3$  which drives the length from 1.5 m to 18 m. Since most of this length is empty space, the only real expense is the greater inductive energy which can be recovered by recirculating the plasma current.

Since the Z-pinch equilibrium is internally balanced (no applied magnetic fields), the optimized design is a smaller plasma radius. This can be seen in Figs. 9 and 10. The figures show the variation away from the

**Table 2. Sample Thruster Parameters for a Flow-Stabilized Z-Pinch**

Entity	$D - He^3$	$p - B^{11}$
$I$ (MA)	5	10
$L$ (m)	10	50
$a$ (mm)	1	1
$T$ (keV)	80	100
$n$ (m <sup>-3</sup> )	$1.5 \times 10^{25}$	$4.7 \times 10^{25}$
$P_f$ (W)	$3.3 \times 10^{12}$	$9.9 \times 10^{12}$
$P_{in}$ (W)	$1.8 \times 10^{12}$	$8.4 \times 10^{12}$
$\dot{m}_{fuel}$ (kg/s)	0.095	0.53
$v_e$ (m/s)	$3.5 \times 10^6$	$1.3 \times 10^6$
$Thrust$ (N)	$3.3 \times 10^5$	$6.8 \times 10^5$

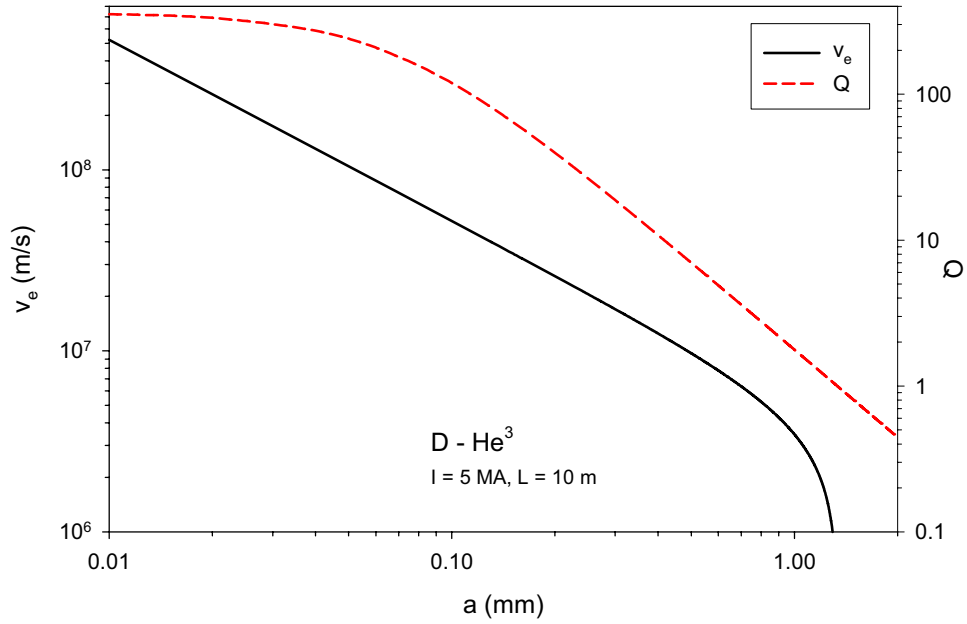


**Figure 9. Thruster parameters for a flow-stabilized Z-pinch operating on the  $D - He^3$  reaction. Notice the maximum permissible pinch radius and the improved performance for smaller pinch radii. The variation of the fusion  $Q$  is also shown.**

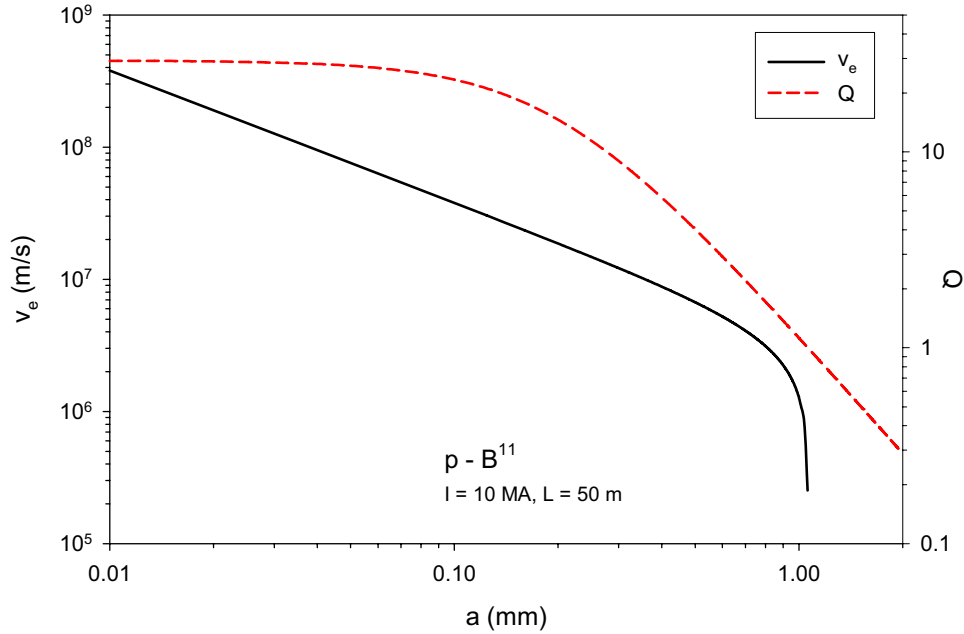


**Figure 10.** Thruster parameters for a flow-stabilized Z-pinch operating on the  $p - B^{11}$  reaction. The parameters are more restrictive than the  $D - He^3$  reaction. Notice the maximum permissible pinch radius and the improved performance for smaller pinch radii. The variation of the fusion  $Q$  is also shown.

point designs in Table 2. For each design there is a maximum permissible pinch radius for the configuration to operate. For each design there is also a maximum fusion  $Q$  which is the ratio of fusion power to input power.

The thruster parameters for the flow-stabilized Z-pinch thruster are in line with the parameters derived by C. H. Williams *et al.*<sup>15</sup> for a fast transfer human mission to Saturn. An important difference is the fusion power for the Z-pinch is larger by approximately  $10^3$  due to its higher plasma density. Additionally, no external field coils are required so the specific power would be much larger as well.

### C. Fusion Burn Simulations of a Z-Pinch

The dynamics of a Z-pinch undergoing fusion burn have been simulated.<sup>7</sup> The simulations solve the time-dependent ideal MHD equations including particle loss (due to fusion) and energy loss (due to fusion, bremsstrahlung radiation, and synchrotron radiation). The plasma is assumed to be in axial equilibrium, or more specifically, the axial gradient length is much larger than the radial gradient length.

The simulations shown here are for  $D + T$  reaction with  $n_D = n_T$  where it is assumed the alpha particles are not confined by the magnetic field. For the simulation parameters,  $r_{L_\alpha} \approx a$ , and the assumption is only marginally satisfied. The plasma current is constant in time. Figure 11 shows the evolution of the particle number density. The number density decreases on axis as fusion burns up the plasma and it is removed from the system. The plasma temperature increases to maintain radial force balance as seen in Fig. 12. The plasma contracts slightly and the plasma pressure profile remains mostly constant. As a result of the increased temperature and hollowed density profile, the fusion reaction rate becomes highest off-axis. See Fig. 13. The primary power loss mechanism is synchrotron radiation which can be seen to maintain a cooler plasma edge where the magnetic field is highest.

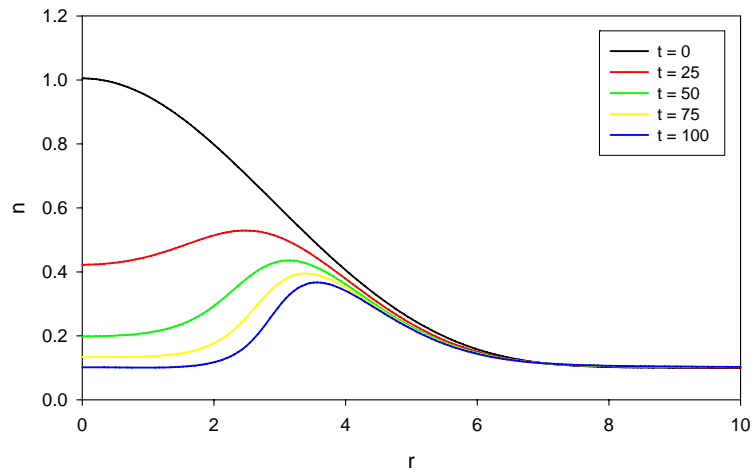


Figure 11. Particle number density evolution for a burning fusion Z-pinch. The number density decreases in the plasma core as the fusion process burns up plasma in the core. Eventually the outer plasma also burns up.

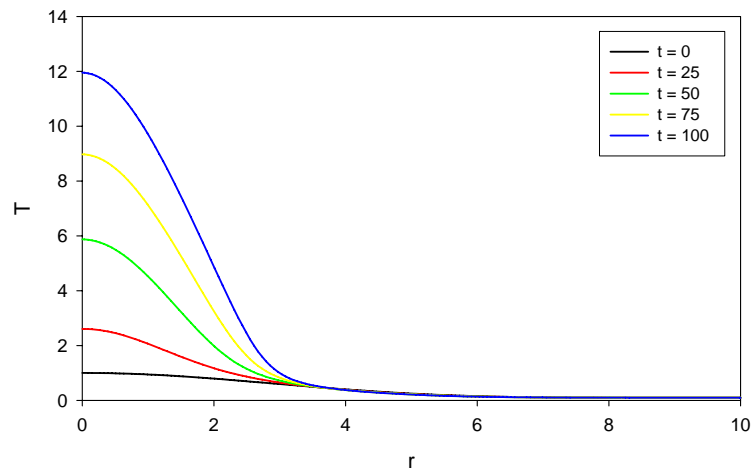
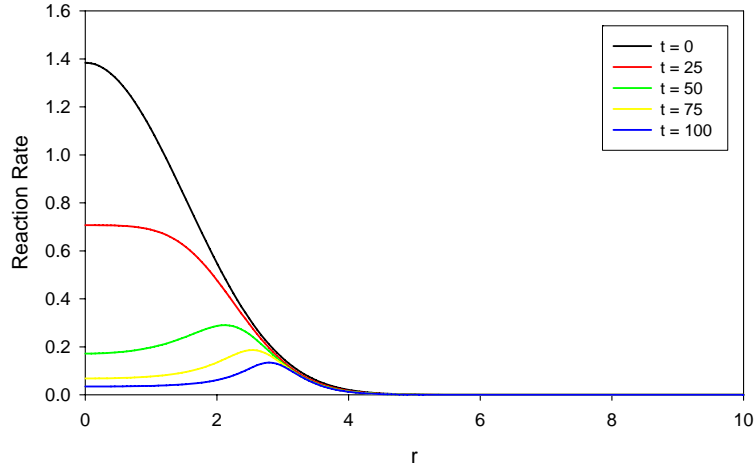


Figure 12. Temperature profile evolution for a burning fusion Z-pinch. Since the plasma current is constant, the temperature must increase as the number density decreases to maintain equilibrium.



**Figure 13. Fusion reaction rate profile evolution for a burning fusion Z-pinch. The combined effect of a hollowing density profile and a rising temperature leads to a reaction rate that is peaked off-axis.**

## V. Conclusions

The Z-pinch has many of the desired features for a fusion space thruster: linear device, no external field coils, high specific power, high plasma density (aneutronic fuels). The problem has always been the gross stability of Z-pinch plasmas. However, using the stabilizing mechanism of sheared flows the Z-pinch may finally have surmounted its most difficult challenge.

The ZaP experiment at the University of Washington may serve as a prototype thruster while it verifies the flow stabilization effect. A fusion space thruster based on the flow-stabilized Z-pinch concept is a near-term prospect that may make manned deep space exploration feasible.

## References

- <sup>1</sup>A. A. Ware, Nucl. Fusion Supp. **3**, 869 (1962).
- <sup>2</sup>B. B. Kadomtsev, *Reviews of Plasma Physics* **2**, 153, New York: Consultants Bureau, 1966.
- <sup>3</sup>M. D. Kruskal and M. Schwarzschild, Proc. R. Soc. London, Sect. A **223**, 348 (1954).
- <sup>4</sup>V. D. Shafranov, At. Energ. [Sov. J. At. Energy] **5**, 38 (1956).
- <sup>5</sup>U. Shumlak, C. W. Hartman, Phys. Rev. Lett. **75** (18), 3285 (1995).
- <sup>6</sup>U. Shumlak, R. P. Golingo, B. A. Nelson, and D. J. Den Hartog, Phys. Rev. Lett. **87** (20), 205005 (2001).
- <sup>7</sup>U. Shumlak, B. A. Nelson, R. P. Golingo, S. L. Jackson, E. A. Crawford, D. J. Den Hartog, Phys. Plasmas **10** (4), 1683 (2003).
- <sup>8</sup>R. P. Golingo, U. Shumlak, and B. A. Nelson, Phys. Plasmas **12** (6), 062505 (2005).
- <sup>9</sup>U. Shumlak, N. F. Roderick, Phys. Plasmas **5** (6), 2384 (1998).
- <sup>10</sup>R. E. Peterkin, Jr., M. H. Frese, and C. R. Sovinec, J. Comput. Phys. **140**, 148 (1998).
- <sup>11</sup>This work is supported by U. S. Department of Energy under Grant DE-FG03-98ER54460.
- <sup>12</sup>R. P. Golingo and U. Shumlak, Rev. Sci. Instrum. **74** (4), 2332 (2003).
- <sup>13</sup>C. W. Hartman, J. L. Eddleman, A. A. Newton, L. J. Perkins, and U. Shumlak, Plasma Phys. **17** (5), 267 (1996).
- <sup>14</sup>C. W. Hartman, J. L. Eddleman, R. Moir, and U. Shumlak, Fusion Tech. **26** (3), 1203 (1994).
- <sup>15</sup>C. H. Williams, S. K. Borowski, L. A. Dudzinski, A. J. Juhasz, AIAA 99-2704, June 1999.
- <sup>16</sup>R. C. Lilly, "Study on a Flow-Through Z-Pinch Fusion Concept," M. S. Thesis, University of Washington, 2006.